

Effective control point layout for boundary surface control method based on the eigenfunction of the internal Dirichlet problem

Tomohiko Ise^{1,2}, Yukio Iwaya¹, and Yôiti Suzuki¹

¹Research Institute of Electrical Communication and Graduate School of Information Sciences, Tohoku University, 2-1-1 Katahira, Aoba-ku, Sendai, 980-8577 Japan

²Alpine Electronics Incorporation, 20-1 Yoshima Industrial Park, Iwaki, 970-1192 Japan

(Received 21 November 2011, Accepted for publication 25 March 2012)

Keywords: Eigenfunction, Global sound reproduction, Boundary surface control, Spatial sampling theory, Internal Dirichlet problem

PACS number: 43.38.VK, 43.55.Br, 43.60.Pt [doi:10.1250/ast.33.322]

1. Introduction

In a small enclosed sound field surrounded by parallel rigid walls, such as a vehicle cabin, strong reflective sounds and standing waves caused by the walls often may cause the degradation of the acoustical transfer function and large differences in the acoustical transfer functions among listening positions. To solve this problem, many methods have been proposed in past studies. In such studies, the multiple point control method, which is based on inverse filters of the acoustical transfer functions among control points and sound sources, seems to be the first attempt [1]. However, in the control of a large area by this multiple point control method, a large number of control points is required and thus the control system size becomes very large. There was another proposal called the boundary surface control (BoSC) method [2]. This method is based on the Kirchhoff-Helmholtz integral equation and can control the entire enclosed area inside a boundary surface only by controlling the sound pressures and their gradients on the boundary surface. Therefore, this method has the potential to reduce the number of control points compared with the multiple point control method in the control of a large area. In the practical application of BoSC, often only the sound pressures are controlled, but in such a case, there is the problem that sound reproduction becomes impossible at the eigenfrequencies where the internal Dirichlet problem arises. To solve this problem, the boundary and additional-points sound pressure control (BAPC) method was proposed [3]. In this method, at least one additional point is placed inside the control area. In BoSC and BAPC, the control point interval and number of control points depend on the spatial sampling theory, but further reduction of the control point number is strongly required in practical control systems such as car audio systems.

In this study, we first verify the performance of BAPC to reproduce a low-frequency plane wave sound field in a small-enclosed sound field surrounded by parallel rigid walls. Then we discuss our effective method for reducing the number of control points using the eigenfunction of the internal Dirichlet problem for the same low-frequency plane wave sound field.

2. Plane wave sound field reproduction performance of BAPC in rectangular enclosed sound field

2.1. Principle of boundary surface control

Here we define the volume V area enclosed by the bounding surface S , as shown in Fig. 1(a). There are no sound sources in the V area. The Helmholtz-equation for sound pressure $(\nabla^2 + k^2)p(\mathbf{r}, \omega) = 0$ can be solved in integral form as the Kirchhoff-Helmholtz integral equation,

$$p(\mathbf{x}, \omega) = \iint_S \left[G(\mathbf{r}|\mathbf{x}, \omega) \frac{\partial p(\mathbf{r}, \omega)}{\partial n} - p(\mathbf{r}, \omega) \frac{\partial G(\mathbf{r}|\mathbf{x}, \omega)}{\partial n} \right] \delta S$$

$$\mathbf{x} \in V, \mathbf{r} \in S, \quad (1)$$

where \mathbf{x} is the spatial position in V , \mathbf{r} is the spatial position on boundary surface S , \mathbf{n} is the normal vector of the boundary surface, ω is the angular frequency, and $G(\mathbf{r}|\mathbf{x}, \omega)$ is the free sound field Green function explained as

$$G(\mathbf{r}|\mathbf{x}, \omega) = \frac{\exp(-jk|\mathbf{r} - \mathbf{x}|)}{4\pi|\mathbf{r} - \mathbf{x}|}. \quad (2)$$

From Eq. (1), when sound pressure $p(\mathbf{r}, \omega)$ and its gradient $\partial p(\mathbf{r}, \omega)/\partial n$ on boundary surface S are defined, sound pressure $p(\mathbf{x}, \omega)$ in volume V can be solved. Using this Kirchhoff-Helmholtz integral equation, the BoSC method [2] equalizes the sound pressure and its gradient on the boundary surface of a sound reproduction area to those of a target sound field. However, the requirement to control both sound pressure and its gradient in the BoSC method causes the practical problem of a large number of control points. Therefore, the BAPC method [3] was proposed to reduce the number of control points. In this method, only sound pressures on the boundary surface as well as those of additional control points placed inside of the control area, as shown in Fig. 1(b), are used. The additional control points are used to avoid the out-of-control problem at eigenfrequencies of the internal Dirichlet problem.

2.2. Plane wave sound field reproduction performance of BAPC in rectangular enclosed sound field

To verify the sound field reproduction performance of BAPC, we assume a rectangular enclosure of 2 m × 1.3 m × 0.1 m (Fig. 2) based on the Nelson and Elliott's acoustical model [4]. The control region is a rectangular area of 1.6 m × 0.8 m and the control points are located on the roof height

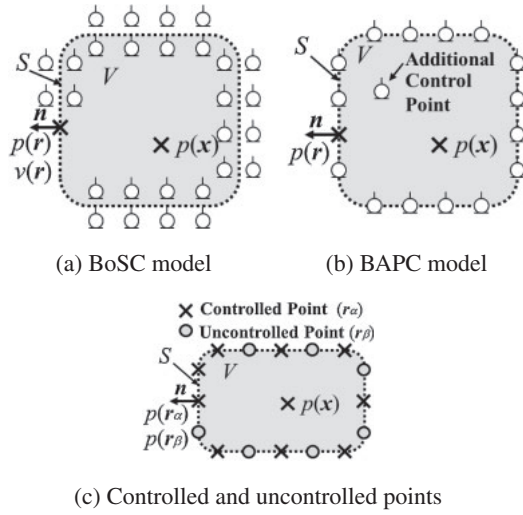


Fig. 1 Sound field model for boundary surface control.

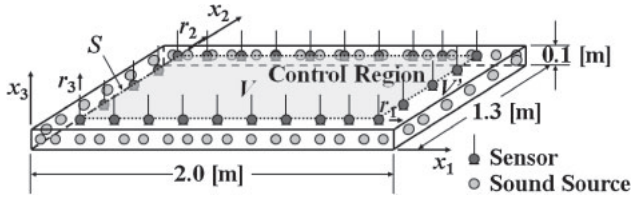


Fig. 2 Control target sound field.

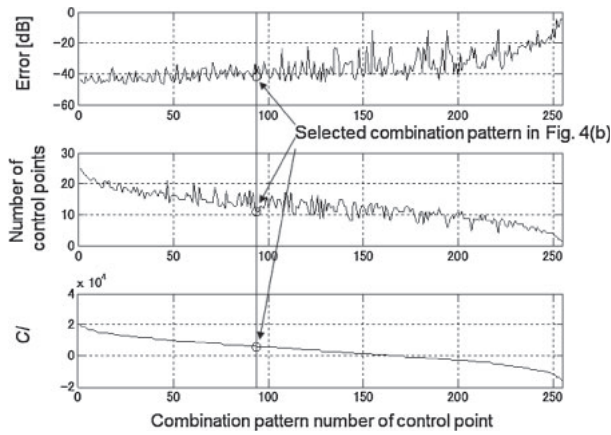
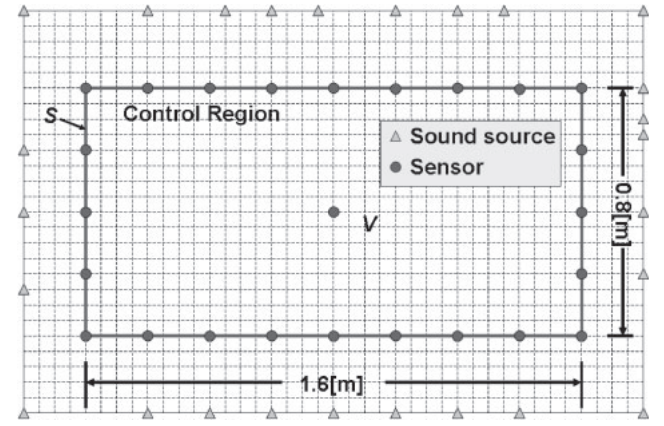
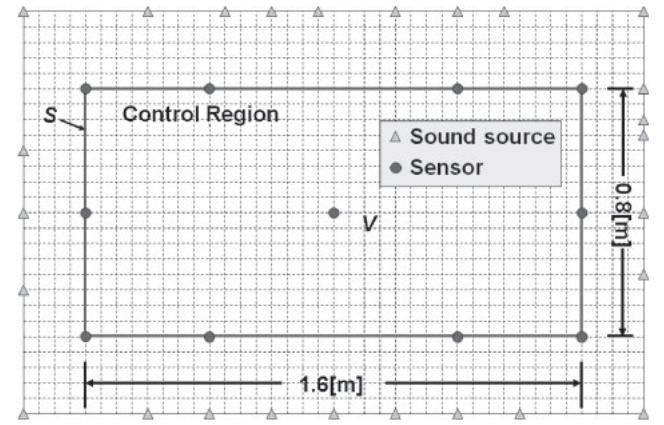


Fig. 3 Control error level and contribution index to combination patterns of control point layout.

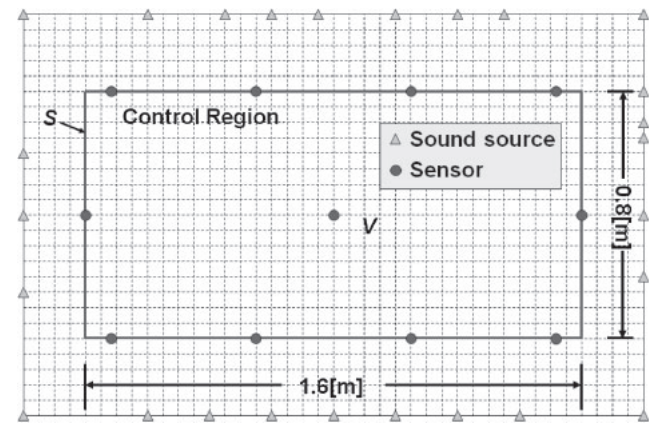
boundary surface with 0.2 m intervals, as shown in Fig. 4(a). It has been shown that an active noise control system based on BoSC achieved a 15 dB reduction with the control point interval of $1/3$ wavelength of the highest control frequency [5], although a control point interval of $1/4$ – $1/6$ wavelength is generally recommended on the basis of spatial sampling theory [6]. Therefore, in the present study, we set the control point interval to within $1/6$ wavelength of the highest control frequency of 250 Hz. The additional control point of BAPC is located at the center of the control region, where there are



(a) Original BAPC layout satisfying spatial sampling theory



(b) Proposed layout



(c) Uniform interval layout

Fig. 4 Layouts of control region, control points and sound sources.

no nodes of eigenfunctions of the internal Dirichlet problem. The total number of control points is set to 25. The sound source layout is selected from 132 positions on the rigid wall at 0.05 m intervals by the Gram-Schmidt orthogonalization method [7], and the number of sound sources is set to 26. The target sound field is set to a plane wave propagating in the x_1 axis direction from front to back.

The dashed-dotted line (a) in Fig. 5 shows the frequency characteristics of the spatial average error level in the control region, which is defined as [3]

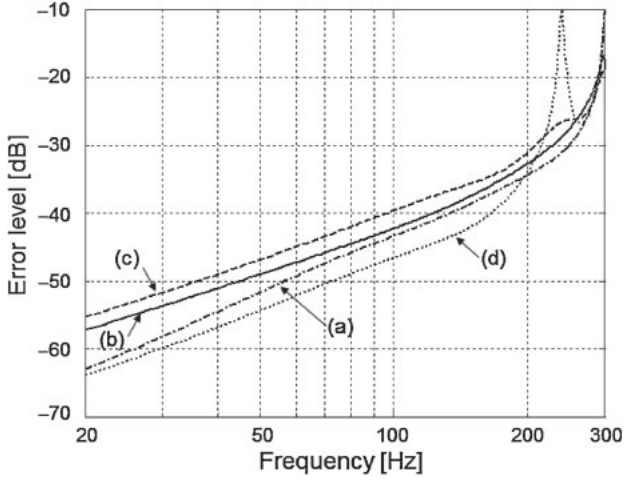


Fig. 5 Average error level in control region. (a) Original BAPC layout satisfying spatial sampling theory (25 control points). (b) Proposed layout (11 control points). (c) Uniform interval layout (11 control points). (d) BAPC without additional control point (24 control points).

$$E(\omega) = 10 \log_{10} \frac{\sum_x |p(\mathbf{x}, \omega) - p_d(\mathbf{x}, \omega)|^2}{\sum_x |p_d(\mathbf{x}, \omega)|^2} \text{ [dB]}, \quad (3)$$

where $p_d(\mathbf{x}, \omega)$ is the target sound pressure. In Fig. 5, the average error levels of the applied BAPC layout are less than -30 dB in the control frequency range up to 250 Hz. This means that BAPC can reproduce the plane wave sound field in the enclosed sound field if the control point layout satisfies the spatial sampling theory [3]. Here, the dotted line in Fig. 5 shows the error levels of BAPC without the additional control point. A clear peak is observed at the eigenfrequency (240 Hz) of the internal Dirichlet problem.

3. Effective control point layout based on eigenfunction of internal Dirichlet problem

3.1. Control point layout index based on eigenfunction of internal Dirichlet problem

As shown in the previous section, BAPC with a control point layout satisfying the spatial sampling theory shows good performance. However, even BAPC, which has smaller system size than that of BoSC, requires many control points to control a large region in practical applications. Therefore we examine an effective method of reducing the number of control points on the basis of the eigenfunction of the internal Dirichlet problem, starting from BAPC with a control point layout satisfying the spatial sampling theory. Control of only sound pressure on the boundary surface means that the boundary condition of the wave equation is defined with only sound pressure. This type of wave equation is called the internal Dirichlet problem. In this case, we can modify the Kirchhoff-Helmholtz integral equation using the internal Dirichlet type Green function $G_D(\mathbf{r}|\mathbf{x}, \omega)$ as

$$p(\mathbf{x}, \omega) = - \iint_S p(\mathbf{r}, \omega) \frac{\partial G_D(\mathbf{r}|\mathbf{x}, \omega)}{\partial \mathbf{n}} \delta S \quad \mathbf{x} \in V, \mathbf{r} \in S, \quad (4)$$

where the gradient of the internal Dirichlet-type Green function is

$$\frac{\partial G_D(\mathbf{r}|\mathbf{x}, \omega)}{\partial \mathbf{n}} = \sum_{\xi} \frac{1}{(k_{\xi}^2 - k^2)V} \frac{\partial \phi_{\xi}(\mathbf{r})}{\partial \mathbf{n}} \phi_{\xi}(\mathbf{x})^*, \quad (5)$$

$$\phi_{\xi}(\mathbf{r}) = \phi_{\xi_1}(r_1) \phi_{\xi_2}(r_2) \phi_{\xi_3}(r_3), \quad (6)$$

$$\phi_{\xi_i}(r_i) = \begin{cases} \sin(\xi_i \pi r_i / L_{Di}) & \xi_i \neq 0 \\ 1 & \xi_i = 0 \end{cases}, \quad (7)$$

where ϕ_{ξ} is the eigenfunction of the ξ th eigenmode. In Eq. (4), boundary surface S separates into controlled points \mathbf{r}_{α} and uncontrolled points \mathbf{r}_{β} , as shown in Fig. 1(c), whereby Eq. (4) is rewritten as

$$p(\mathbf{x}, \omega) = - \iint_{S(\mathbf{r}_{\alpha})} p(\mathbf{r}, \omega) \frac{\partial G_D(\mathbf{r}|\mathbf{x}, \omega)}{\partial \mathbf{n}} \delta S - \iint_{S(\mathbf{r}_{\beta})} p(\mathbf{r}, \omega) \frac{\partial G_D(\mathbf{r}|\mathbf{x}, \omega)}{\partial \mathbf{n}} \delta S. \quad (8)$$

Moreover, the control error $e(\mathbf{x}, \omega)$ can be written as Eq. (9) using the target sound pressures of the boundary surface $p_d(\mathbf{r}, \omega)$ and the control region $p_d(\mathbf{x}, \omega)$,

$$e(\mathbf{x}, \omega) = p_d(\mathbf{x}, \omega) - p(\mathbf{x}, \omega) = - \iint_{S(\mathbf{r}_{\alpha})} (p_d(\mathbf{r}, \omega) - p(\mathbf{r}, \omega)) \frac{\partial G_D(\mathbf{r}|\mathbf{x})}{\partial \mathbf{n}} \delta S - \iint_{S(\mathbf{r}_{\beta})} (p_d(\mathbf{r}, \omega) - p(\mathbf{r}, \omega)) \frac{\partial G_D(\mathbf{r}|\mathbf{x})}{\partial \mathbf{n}} \delta S. \quad (9)$$

From the right side of Eqs. (8) and (9), we could minimize the influence of an uncontrolled boundary surface by applying a control point layout that takes the large numerical value of the first term gradient of the Green function and the small numerical value of the second term gradient of the Green function. In Eq. (5), as the dependence term of \mathbf{r} is $\partial \phi_{\xi}(\mathbf{r}) / \partial \mathbf{n}$, we use this term for the contribution index. Furthermore, we discuss the effect of the sound pressure difference term $p_d(\mathbf{r}, \omega) - p(\mathbf{r}, \omega)$ on the control error in Eq. (9). The sound pressure difference approaches zero at the control points, but generally have certain values at the uncontrolled boundary surface. Therefore, we must estimate the sound pressure difference at the uncontrolled points on the boundary. Thus, we follow Nelson and Elliott's study, i.e., the error of the sound pressure power as a function of the distance from the control point is estimated as being proportional to $1 - \text{sinc}^2(\omega \Delta \mathbf{r} / c_0)$ [8]. On the basis of this estimation, the sound pressure difference is expressed by the following equation: $\sqrt{1 - \text{sinc}^2(\omega \Delta \mathbf{r} / c_0)}$. From the above considerations, we propose a contribution index (CI) of a control point layout as

$$CI = \sum_{\omega} \left\{ \sum_{\mathbf{r}_{\alpha}} \sum_{\xi} \left| \frac{\partial \phi_{\xi}(\mathbf{r}_{\alpha})}{\partial \mathbf{n}} \right| \right\}$$

$$-\sum_{r_\beta} \sum_{\xi} \left| \sqrt{1 - \text{sinc}^2(\omega \Delta \mathbf{r}/c_0)} \frac{\partial \phi_{\xi}(\mathbf{r}_\beta)}{\partial \mathbf{n}} \right|. \quad (10)$$

3.2. Verification of control point layout index

In this section, we verify the correlation between the *CI*s and the performances of sound field reproduction derived by computer simulation. We choose the BAPC system shown in Fig. 4(a) as the starting point of this verification and another shown in Fig. 4(b) as the BAPC system with a reduced number of control points. The numbers of eigenmodes are $\xi_1 = [2, 1, 0]$ for the x_1 axis and $\xi_2 = [1, 0]$ for the x_2 axis. For the control error index, we apply Eq. (11), which is the frequency average of $E(\omega)$ defined by Eq. (3):

$$EF_{\text{ControlPointCombination}} = \sum_{\omega} \frac{E(\omega)}{\Omega}, \quad (11)$$

where Ω is the bandwidth of controlled angular frequency. Here the purpose of this simulation is to confirm the tendency of the influence of the numerical values of eigenfunctions. Therefore, in determining the control point layout, a set of symmetrical control points of an eigenfunction (sine function), which has the same absolute numerical value of $\partial \phi_{\xi}(\mathbf{r})/\partial \mathbf{n}$, is added or removed at the same time. Thus, the four corner points of the control area are treated as one set. Lastly, the 255 combination patterns of the control point layout are chosen for the examination.

The results of the computer simulation are shown in Fig. 3. The bottom graph shows the *CI* defined by Eq. (10) for the 255 combination patterns of the control point layout. Please note that the combination patterns are sorted in descending order of *CI*s. The middle and top graphs respectively show the number of control points and the control errors defined by Eq. (11). Figure 3 shows that the control errors (top graph) and the number of control points (middle graph) tend to become large and small, respectively, as *CI* decreases.

3.3. Verification of control performance with effective control point layout

Here, the performances of the two control point layouts shown in Figs. 4(b) and (c) are examined. The eleven control points shown in Fig. 4(b) were chosen as those having the largest *CI* values in eleven control point combinations, as indicated in Fig. 3 in accordance with the discussion in section 3.1. The eleven control points on the boundary surface have nonuniform distribution and the maximum distance between adjacent control points is 0.8 m, which is longer than half the wavelength of the maximum control frequency of 250 Hz. Therefore, the spatial sampling theory is not satisfied. In contrast, the layout shown in Fig. 4(c) has a constant interval of 0.48 m over the boundary surface.

Figure 5 shows the error levels as a function of frequency for the three layouts shown in Fig. 4. The dashed-dotted line shows the error levels for the original BAPC layout satisfying the spatial sampling theory (Fig. 4(a)). The solid line and the dashed line respectively show the error levels for the proposed nonuniform layout (Fig. 4(b)), and the layout with a uniform interval (Fig. 4(c)). Both layouts have a reduced number of control points of eleven. The degradation, i.e., increase of error levels, of the proposed layout result over the original BAPC layout is 2–6 dB with less than half the number of control points as in the original BAPC. The proposed layout result shows a performance better by about 2–3 dB than that of the uniform interval layout with the same number of control points of eleven. Moreover, the degradation becomes smaller for higher frequencies in both methods, and this tendency is desirable for practical systems.

4. Conclusion

In this paper, we discussed the efficient control point layout for low-frequency plane wave sound field reproduction. We proposed to set the control point layout such that it shows large gradient of the eigenfunction of the internal Dirichlet problem. The control point layouts determined by this tactic showed about 2–3 dB better performance than those with uniform distribution with the same number of control points of eleven.

References

- [1] P. A. Nelson, H. Hamada and S. J. Elliott, "Adaptive inverse filters for stereophonic sound reproduction," *IEEE Trans. Signal Process.*, **40**, 1621–1632 (1992).
- [2] S. Ise, "A principle of sound field control based on the Kirchhoff-Helmholtz integral equation and the theory of inverse systems," *Acta Acustica*, **85**, 78–87 (1999).
- [3] S. Takane, Y. Suzuki and T. Sone, "A new method for global sound field reproduction based on Kirchhoff's integral equation," *Acta Acustica*, **85**, 250–257 (1999).
- [4] P. A. Nelson and S. J. Elliott, *Active Control of Sound* (Academic Press, London, 1992), pp. 311–316.
- [5] T. Nakashima and S. Ise, "A theoretical study of the discretization of the boundary surface in the boundary surface control principle," *Acoust. Sci. & Tech.*, **27**, 199–205 (2006).
- [6] S. Ise, "Application of the boundary surface control principle to the active noise control," *J. Acoust. Soc. Jpn. (J)*, **59**, 414–419 (2003) (in Japanese).
- [7] F. Asano, Y. Suzuki and D. C. Swanson, "Optimization of control source configuration in active control systems using Gram-Schmidt orthogonalization," *IEEE Trans. Speech Audio Process.*, **7**, 213–220 (1999).
- [8] P. A. Nelson and S. J. Elliott, *Active Control of Sound* (Academic Press, London, 1992), pp. 362–366.